Sampling variability under extreme skewness: sample size guidance for future methane measurement campaigns

William S. Daniels[1,2], Dorit M. Hammerling[1,3]

[1]Colorado School of Mines, Golden CO, USA
[2]Current Affiliation: Johns Hopkins University, Baltimore MD, USA
[3]Energy Emissions Modeling and Data Lab, The University of Texas at Austin, Austin TX, USA

Corresponding author: William Daniels
Email: wdanie16@jh.edu

Sampling variability under extreme skewness: sample size guidance for future methane measurement campaigns

William S. Daniels[*,†,‡] and Dorit M. Hammerling[†,¶]

†*Department of Applied Mathematics and Statistics, Colorado School of Mines, Golden, Colorado 80401, United States*

‡*Current Affiliation: Department of Environmental Health and Engineering, Johns Hopkins University, Baltimore, Maryland 21218, United States*

¶*Energy Emissions Modeling and Data Lab, The University of Texas at Austin, Austin, Texas 78712, United States*

* E-mail: wdanie16@jh.edu

Abstract

Methane emissions from the oil and gas sector follow highly right-skewed distributions, making it hard to accurately quantify average emissions with a limited number of measurements. In this study, we probe the statistical implications of sampling (i.e., measuring) from these highly right-skewed distributions, using six US oil and gas basins as an example. For each basin, we provide a minimum sample size that bounds error in the average emission rate estimate introduced by sampling variability. We find that the largest emissions drive sample behavior, and by extension, sample size requirements; samples will underestimate (overestimate) average emissions if super-emitters are observed below (above) their true frequency. Importantly, we show that very large sample sizes can be necessary to mitigate this sampling effect. Furthermore, we find that a one-size-fits-all sampling strategy across basins is suboptimal; differences in super-emitter characteristics between basins necessitate a more tailored sampling approach. To increase the practical applicability of this study, we provide a web tool that both reproduces our findings and performs the same analysis on any user-uploaded distribution of emission rates; the flexibility of this tool enables highly targeted sample size guidance. This work has broad utility across fields where samples are taken from right-skewed distributions.

Introduction

Methane is a potent greenhouse gas with a relatively short lifetime in the atmosphere;[1] this makes reducing methane emissions a key component of short-term climate action.[2,3] The oil and gas sector accounts for 21% of global anthropogenic methane emissions[4] and is viewed as a tractable opportunity for emission reduction.[5] Methane emissions represent a loss of product for many oil and gas operators, providing an economic motivation for emission reduction. Furthermore, certain emission sources within the oil and gas supply chain have clear mitigation pathways: emissions from malfunctioning equipment can often be eliminated once the leaks are identified and engineering improvements can reduce emissions from normally operating equipment like pneumatic controllers.[5]

Traditional activity-based, bottom-up estimates of methane emissions from the oil and gas sector are known to underestimate total emissions.[6–10] As such, efforts to reduce oil and gas methane emissions increasingly rely on direct measurements from ground-based, aerial, or satellite platforms.[11] One such effort is the creation of measurement-based emissions inventories, in which direct measurements are used to estimate, e.g., annual total emissions from a given oil and gas basin.[12] However, due to the distributed nature of oil and gas infrastructure, it is extremely challenging to measure methane at all possible source locations within a basin continuously throughout the year; in practice, any measurement-based inventory of methane emissions is created using a sample of measurements that lacks complete coverage in time or across sites (or both). As such, total emissions are often estimated by extrapolating an average emission rate from a limited sample of measurements (the "sample mean") to the temporal and spatial scale of the measurement-based inventory.[13] This extrapolation introduces uncertainty in the inventory, raising a key question for future measurement campaigns: how large of a sample is necessary to keep error in the sample mean introduced by sampling variability below an acceptable threshold? In other words, how many sites in a basin must be measured to obtain an accurate measurement-based inventory for that basin?

Determining an appropriate sample size is complicated by the fact that methane emissions from the oil and gas sector follow highly right-skewed distributions. In particular, we know from previous campaigns that methane emissions at a single point in time (e.g., from an aerial or satellite technology) across many sites follow a right-skewed distribution.[10,14–18] This is likely because methane emissions over time on individual sites also follow a right-skewed distribution.[19–22] The difference between measurements over time on a single site and at a single point in time over many sites is irrelevant for sample statistics (e.g., the sample mean) if methane emissions follow an ergodic process.[12] However, no study (to our knowledge) has tested this assumption, as doing so requires dense coverage both in time and across sites. We do not test the ergodic assumption in this paper and instead illustrate findings that apply to both samples over time on a single site (e.g., from continuous monitoring systems) and samples at a single point in time over many sites (e.g., from an aerial or satellite technology).

Importantly, samples from right-skewed distributions do not behave in the same way as samples from distributions with minimal skew. Principle among these differences is the rate at which the sample mean converges to a normal distribution, a property guaranteed by the central limit theorem. In the absence of skew, the distribution of sample means (i.e., the distribution obtained by taking the mean of many repeated samples) is approximately normal even if the sample size is small.[23] If the underlying distribution is skewed, however, then a much larger sample size is necessary for the sample mean to approximately follow a normal distribution.[24] In fact, the Berry–Esseen theorem states that the rate of this convergence is

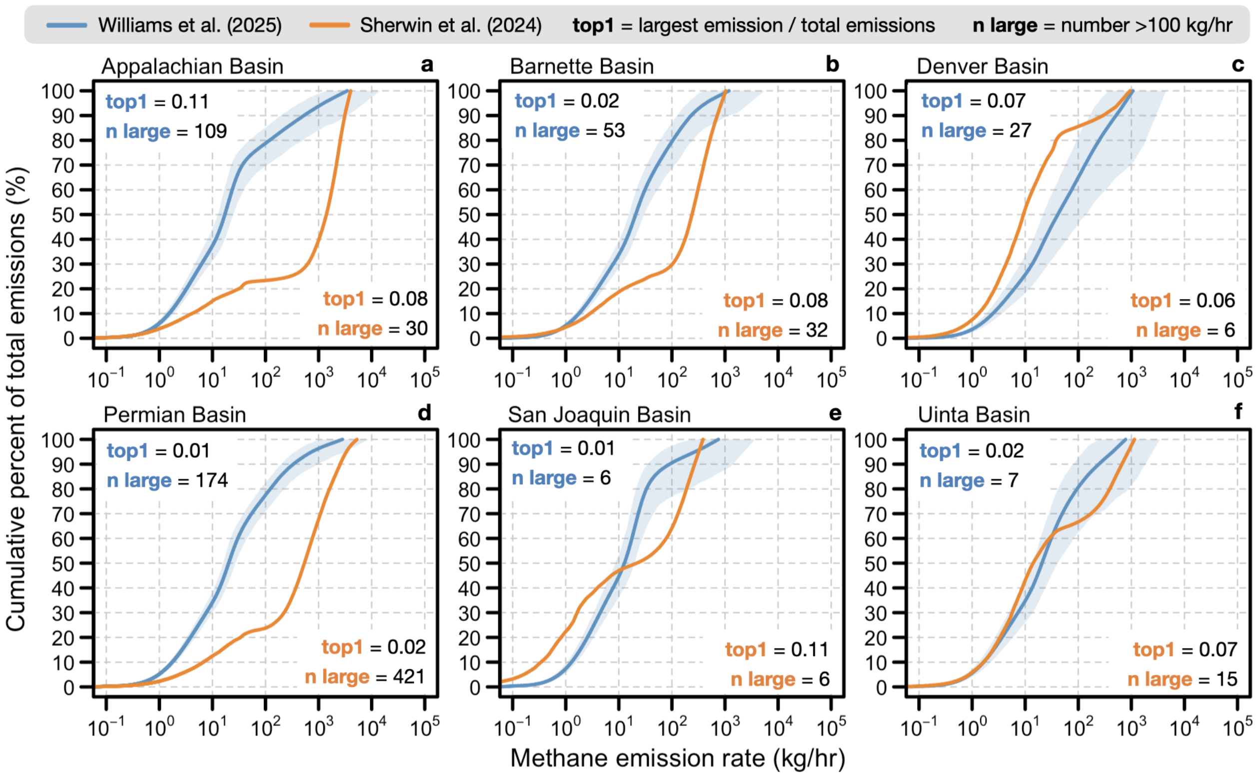

Figure 1: (a) thru (f) The basin-level emission rate distributions used in this study. Williams et al.[26] provide 500 realizations of each distribution; the inner 95% of these realizations is plotted as a shaded region and the average as a solid line. Sherwin et al.[10] provide multiple distributions for each basin that each correspond to a separate measurement campaign; the campaign that most closely aligns in time with the Williams et al.[26] distribution is selected for use in this study. See the Supporting Information file for details. Two metrics related to the largest emissions are shown for each reference distribution; "top1": the magnitude of the largest emission relative to the sum of all emissions ("total emissions"), and "n large": the number of super-emitters (emissions >100 kg/hr).

a direct function of skewness.[25] As a result, many common practices that assume normality of the sample mean cannot be used when analyzing highly right-skewed methane emissions; doing so may misrepresent average emissions or underestimate uncertainty.[17]

In this article, we quantify some of the statistical implications of sampling from highly right-skewed methane emission rate distributions. We then provide basin-specific sample size guidance for future methane measurement campaigns that bounds error in the sample mean caused by sampling variability. We conduct this analysis for six United States oil and gas basins by taking many repeated samples from two state-of-the-art emission rate distributions: Williams et al.[26] and Sherwin et al.[10]. These distributions are shown in Figure 1. The basin-level data provided by these studies allow for basin-specific sample size guidance, expanding previous analysis in Brandt et al.[17]. Additionally, using both sets of reference distributions provides a novel comparison of these contemporary estimates of methane emissions from the US oil and gas sector.[10,26] Finally, we provide a user-friendly web tool that performs the resampling analysis from this paper. This tool can be used to both reproduce our findings using the Williams et al.[26] and Sherwin et al.[10] distributions and to conduct the same analysis on any user-uploaded distribution of emission rates or on a selection of parametric distributions. Using this tool, our sample size guidance can be made more specific to a subregion or collection of sites where users have information a priori about the distribution of emission rates.

Results

Behavior of the sample mean under extreme skewness

Figure 2a illustrates a defining feature of highly right-skewed emission rate distributions: small samples that include rare, extremely large emissions will substantially overestimate the true population mean, while the majority of samples that do not contain these large emissions will slightly underestimate. Figure 2a shows the emission rate distribution from Sherwin et al.[10] for the Denver-Julesburg basin (n = 7,000) and three samples of size n = 200 taken without replacement. This distribution is used for illustrative purposes in Figure 2; basin-specific sample size guidance is provided later in this section. In Figure 2a, Sample 2 includes the largest emission in the population distribution (942 kg/hr) and its mean consequently overestimates the true mean by an order of magnitude. This is because Sample 2 is not large enough to contain a sufficient number of small emissions to average out the influence of the largest emission. Samples 1 and 3 do not include the largest emissions and, as a result, underestimate the true average emission rate.

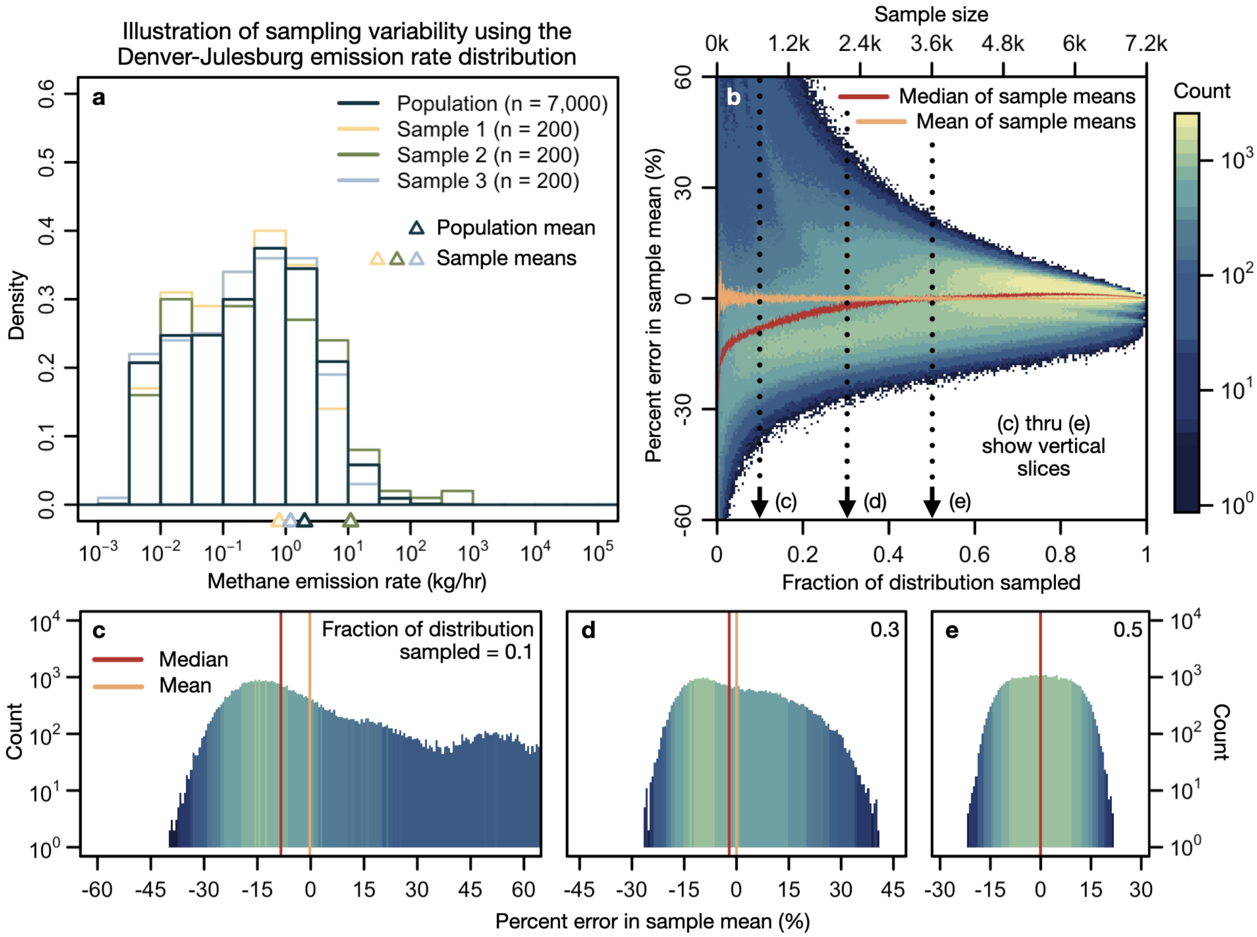

Figure 2: Illustration of sampling variability using the Denver-Julesburg emission rate distribution from Sherwin et al.[27]. (a) Population distribution and three samples of size n = 200 plotted on a log-scale. Average values are shown as triangles along the horizontal axis. (b) Distribution of 1,000 repeated sample means (shown as percent errors) at sample sizes ranging from one to the length of the population distribution. The bottom axis shows sample size as a fraction of the length of the distribution, and the top axis shows sample size as a number of measurements. The color scale shows the number of samples within each grid cell. (c) thru (e) Three vertical "slices" from (b) at different sample sizes (equivalently, different sampled fractions). Both vertical axis and color scale show the number of samples within each percent error bin. Note that the mean and median are visually the same in (e).

Figure 2b shows the behavior of 1,000 samples taken at sample sizes ranging from a single measurement to the size of the full distribution. These samples were again taken without replacement; see the Methods section for a discussion of this choice. Figures 2c thru e show three vertical "slices" from Figure 2b as histograms. For the Denver-Julesburg basin, a surprisingly large sample is required to mitigate the influence of the rare super-emitters. Sampling 50% of the distribution (the threshold for comprehensive spatial coverage in Sherwin et al.[10]) results in a 95% confidence interval for the sample mean between -15.0% and 15.3% of the true mean and a maximum error of 23.0% in the sample mean. Note that the median becomes slightly positive when sampling over 50% of the distribution; this behavior is explained in the following section.

Smaller samples amplify the effects of sampling variability: with a sample of size n = 200 (as used in Figure 2a), the 95% confidence interval for the sample mean is between -40.5% and 209.6% and the maximum error is 378.5%. Furthermore, at this sample size, there is a 72% chance that the sample mean will underestimate by failing to capture the rare, large emissions in the population distribution. In summary, for the Denver-Julesburg basin (according to the Sherwin et al.[10] distribution), measuring 200 sites results in substantial variability in the sample mean, and even a relatively large sample covering half of the basin is not enough to fully mitigate these sampling effects.

We pause here to highlight two important points. First, errors of the magnitude seen in Figure 2 are not uncommon in individual emission rate estimates, regardless of the measurement technology (e.g., ground-based, aerial, satellite).[27–31] However, the percent errors in Figure 2 are in the *mean* of many emission rate estimates, with sample sizes ranging from one to the length of the full distribution. Second, the behavior of the sample mean shown in Figure 2 is not a result of *bias* in the sample mean; the sample mean is an unbiased estimator of the population mean by definition.[23] As such, the mean of many repeated sample means will equal the true population mean (seen in Figure 2). However, in practice it is often infeasible to take many repeated samples, making it important to understand the behavior of an individual sample under different sample sizes and super-emitter regimes.

Impact of super-emitters on sampling variability

Figure 3 highlights the outsized influence of super-emitters on sampling variability. Again using the Denver-Julesburg distribution from Sherwin et al.[10], Figure 3 shows three error

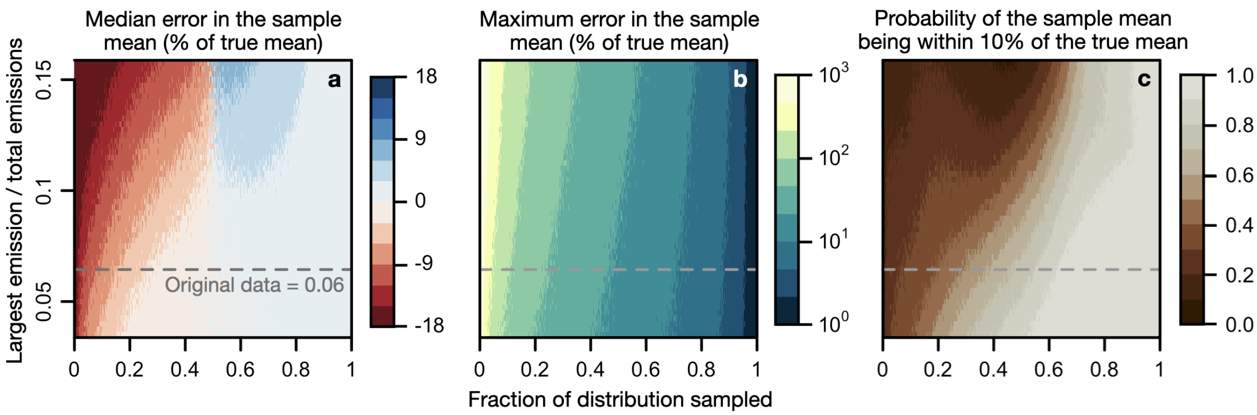

Figure 3: Impact of the largest emission in the population distribution on sampling variability. The subplots show three error metrics for the sample mean using the Denver-Julesburg emission rate distribution from Sherwin et al.[10] as an example. The horizontal axis shows sample size as a fraction of the population. The vertical dimension shows how the error metrics change as the magnitude of the largest emission in the population distribution is adjusted. The vertical axis gives the magnitude of the largest emission in the population distribution relative to total emissions. The true ratio of largest emission to total emissions for the Sherwin et al.[10] Denver-Julesburg basin is shown as a horizontal dashed line. All other rows are generated by artificially replacing the largest emission with a different value and taking new samples.

metrics for the sample mean across a range of sample sizes and as the magnitude of the largest emission in the population distribution changes. We manually adjust the largest emission in the Sherwin et al.[10] distribution to illustrate this behavior.

At sample sizes below 50% of the distribution, the sample mean becomes more likely to underestimate as the largest emission increases (Figure 3a). This is because average (or, equivalently, cumulative) emissions are sensitive to outliers, making it increasingly necessary to observe the largest emission as its magnitude, and therefore influence on the mean, increases. Interestingly, sample sizes above 50% have a slight tendency to overestimate. This is because these samples are all more likely to observe the largest emission than to miss it, and once the largest emission is observed, a large number of "normal" emissions closer to the bulk of the distribution must be observed to counteract its influence.

A single sample becomes less likely to be within 10% of the true mean as the magnitude of the largest emission in the underlying distribution increases (Figure 3c). This metric is particularly important for determining the sample size of future measurement campaigns, as a campaign provides just one "sample" from the true emission rate distribution. As seen in Figure 3c, it becomes increasingly necessary to measure almost all sites within a basin as the magnitude of the largest emission increases relative to total emissions.

Basin-specific sample size guidance

Figure 4 provides sample size guidance for future methane measurement campaigns in six US oil and gas basins based on three error metrics related to the sample mean. For each metric, we show the sample size required to keep the error introduced by sampling variability below a given threshold. The specific thresholds shown in Figure 4 are not meant to be an exhaustive list, rather they are meant to demonstrate how sample size requirements vary by basin, reference distribution, and error tolerance.

We highlight three findings from Figure 4. First, the behavior of the largest emissions drives sampling variability and, by extension, sample size requirements across the three error metrics studied here. In particular, the magnitude of the largest emission in the true population distribution relative to total emissions is a significant predictor ($p < 0.01$) of required sample size based on a simple linear regression for all three error metrics. This is a direct result of the behavior shown in Figure 3: the presence of super-emitters that are both large and rare make it hard to accurately characterize average emissions. Interestingly, basins with more super-emitters (>100 kg/hr) require smaller samples to accurately characterize average emissions. This is because a measurement campaign is more likely to observe super-emitters in basins where they are more common, like the Permian, than in basins where they are relatively rare, like the Denver-Julesburg. As a result, it easier to characterize both the bulk and the tail of the emission rate distribution in the Permian, leading to a more accurate estimate of average emissions at smaller sample sizes. This fact has important implications for measurement campaign design; if the objective is to detect as many super-emitters as possible (e.g., for emission mitigation), then it is desirable to allocate more measurements to basins with more super-emitters. Conversely, if the objective is to characterize average emissions as accurately as possible (e.g., for inventory development), then it is desirable to allocate more measurements to basins with fewer super-emitters where they are harder to find.

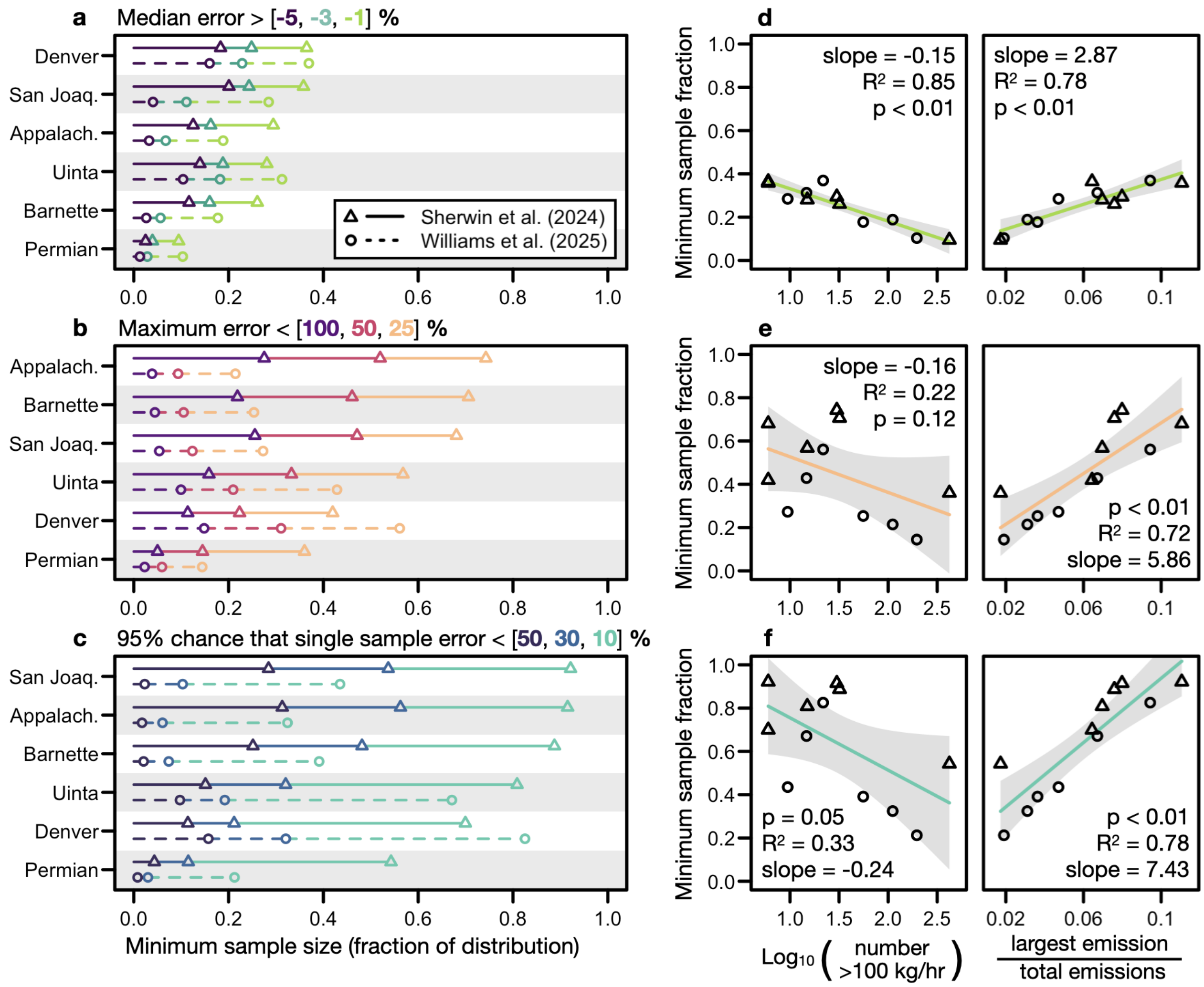

Figure 4: Basin-specific sample size guidance according to three different error metrics for the sample mean: (a) median error, (b) maximum error, and (c) single sample error. Each point shows the minimum sample size fraction required to satisfy the corresponding error threshold listed in the plot title. Correspondence between points and error thresholds is shown with color. Point and line type denote the reference distribution. Basins on the vertical axis are sorted according to the Sherwin et al.[10] values within each plot. (d) thru (f) Linear relationship between two features of the emission rate distributions and the sample size required to meet the strictest error thresholds from (a) thru (c). Each point corresponds to a basin-level distribution from either Williams et al.[26] or Sherwin et al.[10]. Vertical axis shows the sample size required to satisfy the strictest error threshold from (a) thru (c), and the horizontal axes shows the feature values: the base-10 logarithm of the number of super emitters (>100 kg/hr) and the magnitude of the largest emission relative to total emissions.

Second, despite variability between basins, very large samples are often required to keep the error in a single sample below 10% (at the 95% confidence level). As stated above, this is an important metric for measurement campaign design, as each campaign provides one "sample" of the emission rate distribution at a snapshot in time. For example, when using the Sherwin et al.[10] distributions, campaigns must measure over 80% of sites in the San Joaquin, Appalachian, Barnette, and Uinta basins to keep the error in a single sample below 10% (at the 95% confidence level). When using the Williams et al.[26] distributions, campaigns must measure over 80% of sites in the Denver-Julesburg basin to meet the same error threshold.

Third, as illustrated by the previous example, there are substantial differences between the Williams et al.[26] and Sherwin et al.[10] emission rate distributions. In particular, the Williams et al.[26] distributions have a larger contribution from emissions <100 kg/hr than the Sherwin et al.[10] distributions in all but the Denver-Julesburg basin. Similarly, the Sherwin et al.[10] distributions have a larger contribution to total emissions from the single largest emission than the Williams et al.[26] distributions in four of the six basins. Because the largest emissions have an outsized influence on the behavior of the sample mean, the Sherwin et al.[10] distributions often have more variability in the sample mean than the Williams et al.[26] distributions, which ultimately results in larger sample size requirements. Given the large difference in sample size requirements between these two sets of distributions, it is clear that more work is needed to definitively characterize the distribution of methane emission rates in US oil and gas basins.

Discussion

Despite recent federal deregulation in the United States, ongoing efforts to measure methane from the US oil and gas sector will likely continue. From an economic perspective, methane emissions often represent a loss of product to oil and gas operators, incentivizing measurement-based surveys to quickly identify leaks. From a reporting perspective, voluntary global programs, such as OGMP 2.0,[32] and recent import requirements set by the European Union[33] both require measurement-based emissions accounting. The latter has demonstrated that participation in parts of the global natural gas market may depend on the ability to measure and verify emission intensities. In addition, measurement-based reporting requirements may resume in the US, such as the methane fee for large release events previously introduced by the US Environmental Protection Agency.[34]

Whether or not they are intended to satisfy the reporting programs discussed above, all future methane measurement campaigns will need to select a sample size. In this study, we have provided specific sample size requirements to bound errors introduced by sampling variability in six US oil and gas basins. We find that sample size requirements vary by basin, largely being driven by differences in super-emitter characteristics between basins. Furthermore, we find notably different sample size requirements when using different reference distributions.[10,26] Improved sample size guidance will require reconciliation of these state-of-the-art estimates of methane emissions from the US oil and gas sector.

To broaden the applicability of this work, we have created a web tool to both reproduce our analysis using the Williams et al.[26] and Sherwin et al.[10] distributions and to perform the same analysis on any user-uploaded distribution or a selection of parametric distributions. Using this tool, sample size requirements can be made more specific to a subregion or collection of sites (e.g., all sites owned by a specific operator) where users have information a priori about the distribution of emission rates. Additionally, this tool can be used to calculate sample size requirements at any user-specified error thresholds, not just the selection of thresholds shown in Figure 4.

Our method for estimating sampling variability, made publicly available in the web tool discussed above, also has broad applicability beyond methane emissions from the oil and gas sector. Any measurement campaign focused on atmospheric pollutants or trace gasses that is unable to visit all possible source locations will need to make a sample size determination. Ignoring the impact of sampling variability for any such campaign may lead to misinterpretation of uncertainties in the downstream analysis.

While the focus of this article was on the distribution of emissions over sites at a single point in time, the methodology (and web tool) are equally applicable for distributions of emissions over time on a single site. In this context, a similar question often emerges: how often do I need to measure a given site to accurately estimate the long-term average emission rate? The answer to this question has implications for, e.g., the number of fixed point sensors that must be installed around the fenceline of a given facility; more sensors mean more coverage but come at a higher cost. As estimates for emission rate distributions over time evolve (e.g., from continuous point sensors), they can be uploaded to the web tool directly for temporal sample size guidance.

Finally, it is important to reiterate that the sample size guidance presented in this study only considers sampling variability. There may be other considerations that contribute to measurement campaign design, such as a desired stratification across facility types.[12,35] Furthermore, this study (intentionally) does not consider variability introduced by temporal intermittency, or the fact that methane emissions vary over time. Other studies have made advancements in this direction by conducting repeat measurement campaigns of the same region, finding that aggregated methane emissions are different (to varying degrees) between repeat campaigns.[10,35] These differences are a result of both temporal variability and sampling variability (because only a subset of sites were measured). By isolating errors in the sample mean caused solely by sampling variability, we provide a way to estimate the contribution of temporal variability alone when conducting repeat measurement campaigns.

Methods

Reference emission rate distributions

Williams et al.[26] used data from 16 studies to create basin-level methane emission rate distributions. Approximately 85% of these data are from site-level measurements using technologies with low detection thresholds around 0.1 kg/hr, such as tracer-based releases, EPA Other Test Method (OTM 33), or Gaussian dispersion modeling. The other 15% of the data are from aggregated component-level measurements, such as Hi-Flow samplers or flux chambers. These measurement data are scaled to the basin-level within a probabilistic framework that leverages activity data and flaring detections.

Sherwin et al.[10] used aerial data from Kairos Aerospace (now Insight M) and Carbon Mapper (CM) together with the bottom-up simulation tool from Rutherford et al.[8] to create methane emission rate distributions at the basin-level. Both Kairos and CM have higher detection thresholds ($\sim$10 kg/hr) than the measurement technologies used in Williams et al.[26]. Sherwin et al.[10] provide multiple distributions per basin, each corresponding to a different measurement campaign. For the analysis in this paper, we select the Sherwin et al.[10] distributions that most closely align in time with the Williams et al.[26] basin-level distributions. See the Supporting Information file for details.

Resampling methodology

For both the Williams et al.[26] and Sherwin et al.[10] emission rate distributions, we resample the data to quantify sampling variability under different sample sizes, roughly following the procedure in Chen et al.[36]. That is, for each of the distributions shown in Figure 1, we sample 1,000 times without replacement at sample sizes ranging from a single measurement to the size of the entire distribution. We then compare the 1,000 sample means to the true distribution mean using three metrics: the median percent error (Q_{50}), the maximum percent error ($\epsilon_{\max}$), and the probability of a single sample being within 10% of the truth ($\mathbb{P}_{10}$). For a given sample size and distribution, if we let $\bar{\boldsymbol{x}}^* = \{\bar{x}_1^*, ..., \bar{x}_{1000}^*\}$ represent the 1,000 sample means and μ the true distribution mean, then we compute the percent error in each sample mean as

$$\boldsymbol{\epsilon} = 100 \times (\bar{\boldsymbol{x}}^* - \mu)/\mu$$

and the three metrics as

$$\mathrm{Q}_{50} = \mathrm{median}(\boldsymbol{\epsilon}), \quad \epsilon_{\max} = \max(\boldsymbol{\epsilon}), \quad \mathbb{P}_{10} = \frac{\text{number of } |\boldsymbol{\epsilon}| < 10}{\text{length of } \boldsymbol{\epsilon}}.$$

We sample without replacement to isolate sampling variability from other causes of variability, such as temporal intermittency. The physical interpretation of this approach depends on whether the true population distribution represents emissions over time on a single site or emissions over sites at a single point in time. For emissions over time, sampling without replacement ensures that the estimate of long-term average emissions approaches the true value as measurements are taken at a higher frequency (and, in the limit, approach a truly continuous measurement system). In this context, sampling 50% of the distribution can be interpreted as measuring emissions half of the time. For emissions over sites, sampling without replacement ensures that measuring all sites results in a correct estimate of average emissions at a snapshot in time, which is the desired behavior if we ignore temporal variability. In this context, sampling 50% of the distribution can be interpreted as measuring half of the sites within a given domain. This paper focuses on the latter situation.

This resampling procedure assumes that the distributions from Williams et al.[26] and Sherwin et al.[10] are the true underlying emission distributions in their respective regions, despite these distributions being (very large) samples themselves. The resampling procedure also assumes that emissions of all sizes can be detected, while in reality all measurement technologies have a probability of detection that decreases with emission magnitude. However, emissions below the detection threshold of the measurement technology can be estimated (usually via a bottom-up inventory) and added to the estimate of total emissions.

Data Availability

Methane emission rate distributions from Sherwin et al.[10] can be obtained from their "Source data" section. Methane emission rate distributions from Williams et al.[26] can be obtained from Williams[37].

Acknowledgments

This work was partially funded through the Energy Emissions Modeling and Data Lab (EEMDL) and the Colorado Ongoing Basin Emissions (COBE) project.

Author Contributions

W.S.D.: Conceptualization, Analysis, Visualization, Writing - Original Draft, Writing - Editing and Review. D.M.H.: Conceptualization, Writing - Editing and Review, Funding Acquisition, Project Supervision.

Competing Interests

The authors have no competing interests to declare.

Supporting Information

- Supporting information file.
- Web tool: `https://mbasanese-sampling.share.connect.posit.cloud/`

References

(1) Szopa, S.; Naik, V.; Adhikary, B.; Artaxo, P.; Berntsen, T.; Collins, W.; Fuzzi, S.; Gallardo, L.; Kiendler-Scharr, A.; Klimont, Z.; Liao, H.; Unger, N.; Zanis, P. Short-Lived Climate Forcers. 2021; In Climate Change 2021: The Physical Science Basis. Contri-

bution of Working Group I to the Sixth Assessment Report of the Intergovernmental Panel on Climate Change. https://doi.org/10.1017/9781009157896.008.

(2) Schleussner, C. F.; Rogelj, J.; Schaeffer, M.; Lissner, T.; Licker, R.; Fischer, E. M.; Knutti, R.; Levermann, A.; Frieler, K.; Hare, W. Science and policy characteristics of the Paris Agreement temperature goal. *Nature Climate Change 2016 6:9* **2016**, *6*, 827–835, https://doi.org/10.1038/nclimate3096.

(3) Collins, W. J.; Webber, C. P.; Cox, P. M.; Huntingford, C.; Lowe, J.; Sitch, S.; Chadburn, S. E.; Comyn-Platt, E.; Harper, A. B.; Hayman, G.; Powell, T. Increased importance of methane reduction for a 1.5 degree target. *Environmental Research Letters* **2018**, *13*, 054003–054003, https://doi.org/10.1088/1748-9326/AAB89C.

(4) International Energy Agency Global Methane Tracker 2025. Paris: International Energy Agency. https://www.iea.org/reports/global-methane-tracker-2025, 2025; CC BY 4.0 License.

(5) Nisbet, E. G. et al. Methane Mitigation: Methods to Reduce Emissions, on the Path to the Paris Agreement. *Reviews of Geophysics* **2020**, *58*, e2019RG000675, https://doi.org/110.1029/2019RG000675.

(6) Alvarez, R. A. et al. Assessment of methane emissions from the U.S. oil and gas supply chain. *Science* **2018**, *361*, 186–188, https://doi.org/10.1126/science.aar7204.

(7) Chan, E.; Worthy, D. E. J.; Chan, D.; Ishizawa, M.; Moran, M. D.; Delcloo, A.; Vogel, F. Eight-Year Estimates of Methane Emissions from Oil and Gas Operations in Western Canada Are Nearly Twice Those Reported in Inventories. *Environmental Science & Technology* **2020**, *54*, 14899–14909, https://doi.org/10.1021/acs.est.0c04117.

(8) Rutherford, J. S.; Sherwin, E. D.; Ravikumar, A. P.; Heath, G. A.; Englander, J.; Cooley, D.; Lyon, D.; Omara, M.; Langfitt, Q.; Brandt, A. R. Closing the methane gap

in US oil and natural gas production emissions inventories. *Nature Communications* **2021**, *12*, 4715, https://doi.org/10.1038/s41467-021-25017-4.

(9) Conrad, B. M.; Tyner, D. R.; Li, H. Z.; Xie, D.; Johnson, M. R. A measurement-based upstream oil and gas methane inventory for Alberta, Canada reveals higher emissions and different sources than official estimates. *Communications Earth & Environment* **2023**, *4*, 1–10, https://doi.org/10.1038/s43247-023-01081-0.

(10) Sherwin, E. D.; Rutherford, J. S.; Zhang, Z.; Chen, Y.; Wetherley, E. B.; Yakovlev, P. V.; Berman, E. S. F.; Jones, B. B.; Cusworth, D. H.; Thorpe, A. K.; Ayasse, A. K.; Duren, R. M.; Brandt, A. R. US oil and gas system emissions from nearly one million aerial site measurements. *Nature* **2024**, *627*, 328–334, https://doi.org/10.1038/s41586-024-07117-5.

(11) Fox, T. A.; Barchyn, T. E.; Risk, D.; Ravikumar, A. P.; Hugenholtz, C. H. A review of close-range and screening technologies for mitigating fugitive methane emissions in upstream oil and gas. *Environmental Research Letters* **2019**, *14*, 053002–053002, https://doi.org/10.1088/1748-9326/AB0CC3.

(12) Johnson, M. R.; Conrad, B. M.; Tyner, D. R. Creating measurement-based oil and gas sector methane inventories using source-resolved aerial surveys. *Communications Earth & Environment* **2023**, *4*, 1–9, https://doi.org/10.1038/s43247-023-00769-7.

(13) Fosdick, B. K.; Weller, Z.; Wong, H. X.; Corbett, A.; Roell, Y.; Martinez, E.; Berry, A.; Gielczowski, N.; Hajny, K. D.; Moore, C. Extrapolation Approaches for Creating Comprehensive Measurement-Based Methane Emissions Inventories. *ChemRxiv* **2025**, https://doi.org/10.31223/X5K14J.

(14) Duren, R. M. et al. California's methane super-emitters. *Nature* **2019**, *575*, 180–184, https://doi.org/10.1038/s41586-019-1720-3.

(15) Frankenberg, C.; Thorpe, A. K.; Thompson, D. R.; Hulley, G.; Kort, E. A.; Vance, N.; Borchardt, J.; Krings, T.; Gerilowski, K.; Sweeney, C.; Conley, S.; Bue, B. D.; Aubrey, A. D.; Hook, S.; Green, R. O. Airborne methane remote measurements reveal heavy-tail flux distribution in Four Corners region. *Proceedings of the National Academy of Science* **2016**, *113*, 9734–9739, https://doi.org/10.1073/pnas.1605617113.

(16) Wang, J. L.; Daniels, W. S.; Hammerling, D. M.; Harrison, M.; Burmaster, K.; George, F. C.; Ravikumar, A. P. Multiscale Methane Measurements at Oil and Gas Facilities Reveal Necessary Frameworks for Improved Emissions Accounting. *Environmental Science & Technology* **2022**, *56*, 14743–14752, https://doi.org/10.1021/ACS.EST.2C06211.

(17) Brandt, A. R.; Heath, G. A.; Cooley, D. Methane Leaks from Natural Gas Systems Follow Extreme Distributions. *Environmental Science & Technology* **2016**, *50*, 12512–12520, https://doi.org/10.1021/acs.est.6b04303.

(18) Cusworth, D. H.; Duren, R. M.; Thorpe, A. K.; Olson-Duvall, W.; Heckler, J.; Chapman, J. W.; Eastwood, M. L.; Helmlinger, M. C.; Green, R. O.; Asner, G. P.; Dennison, P. E.; Miller, C. E. Intermittency of Large Methane Emitters in the Permian Basin. *Environmental Science & Technology Letters* **2021**, *8*, 567–573, https://doi.org/10.1021/acs.estlett.1c00173.

(19) Allen, D. T.; Cardoso-Saldaña, F. J.; Kimura, Y.; Chen, Q.; Xiang, Z.; Zimmerle, D.; Bell, C.; Lute, C.; Duggan, J.; Harrison, M. A Methane Emission Estimation Tool (MEET) for predictions of emissions from upstream oil and gas well sites with fine scale temporal and spatial resolution: Model structure and applications. *Science of The Total Environment* **2022**, *829*, 154277, https://doi.org/10.1016/j.scitotenv.2022.154277.

(20) Daniels, W. S.; Wang, J. L.; Ravikumar, A. P.; Harrison, M.; Roman-White, S. A.;

George, F. C.; Hammerling, D. M. Toward Multiscale Measurement-Informed Methane Inventories: Reconciling Bottom-Up Site-Level Inventories with Top-Down Measurements Using Continuous Monitoring Systems. *Environmental Science & Technology* **2023**, *57*, 11823–11833, https://doi.org/10.1021/acs.est.3c01121.

(21) Khaliukova, O.; Zhu, Y.; Daniels, W. S.; Ravikumar, A. P.; Ross, G. B.; Roman-White, S. A.; George, F. C.; Hammerling, D. M. Investigating Aerial Data Preanalysis Schemes and Site-Level Methane Emission Aggregation Methods at Liquefied Natural Gas Facilities. *ACS ES&T Air* **2025**, *2*, 1009–1019, https://doi.org/10.1021/acsestair.4c00301.

(22) Daniels, W. S.; Kidd, S. G.; Yang, S. L.; Stokes, S.; Ravikumar, A. P.; Hammerling, D. M. Intercomparison of Three Continuous Monitoring Systems on Operating Oil and Gas Sites. *ACS ES&T Air* **2025**, *2*, 564–577, https://doi.org/10.1021/acsestair.4c00298.

(23) Casella, G.; Berger, R. *Statistical Inference*, 2nd ed.; Chapman and Hall/CRC: New York, 2024; https://doi.org/10.1201/9781003456285.

(24) Hastie, T.; Tibshirani, R.; Friedman, J. *The Elements of Statistical Learning*; Springer Series in Statistics; Springer: New York, NY, 2009; https://doi.org/10.1007/978-0-387-84858-7.

(25) Korolev, V. Y.; Shevtsova, I. G. On the Upper Bound for the Absolute Constant in the Berry–Esseen Inequality. *Theory of Probability & Its Applications* **2010**, *54*, 638–658, https://doi.org/10.1137/S0040585X97984449.

(26) Williams, J. P.; Omara, M.; Himmelberger, A.; Zavala-Araiza, D.; MacKay, K.; Benmergui, J.; Sargent, M.; Wofsy, S. C.; Hamburg, S. P.; Gautam, R. Small emission sources in aggregate disproportionately account for a large majority of total methane

emissions from the US oil and gas sector. *Atmospheric Chemistry and Physics* **2025**, *25*, 1513–1532, https://doi.org/10.5194/acp-25-1513-2025.

(27) Sherwin, E. D.; El Abbadi, S. H.; Burdeau, P. M.; Zhang, Z.; Chen, Z.; Rutherford, J. S.; Chen, Y.; Brandt, A. R. Single-blind test of nine methane-sensing satellite systems from three continents. *Atmospheric Measurement Techniques* **2024**, *17*, 765–782, https://doi.org/10.5194/amt-17-765-2024.

(28) Bell, C.; Ilonze, C.; Duggan, A.; Zimmerle, D. Performance of Continuous Emission Monitoring Solutions under a Single-Blind Controlled Testing Protocol. *Environmental Science & Technology* **2023**, *57*, 5794–5805, https://doi.org/10.1021/acs.est.2c09235.

(29) Ilonze, C.; Emerson, E.; Duggan, A.; Zimmerle, D. Assessing the Progress of the Performance of Continuous Monitoring Solutions under a Single-Blind Controlled Testing Protocol. *Environmental Science & Technology* **2024**, *58*, 10941–10955, https://doi.org/10.1021/acs.est.3c08511.

(30) Cheptonui, F.; Emerson, E.; Ilonze, C.; Day, R.; Levin, E.; Fleischmann, D.; Brouwer, R.; Zimmerle, D. J. Assessing the performance of emerging and existing continuous monitoring solutions under a single-blind controlled testing protocol. *Elementa: Science of the Anthropocene* **2025**, *13*, 00020, https://doi.org/10.1525/elementa.2025.00020.

(31) El Abbadi, S. H.; Chen, Z.; Burdeau, P. M.; Rutherford, J. S.; Chen, Y.; Zhang, Z.; Sherwin, E. D.; Brandt, A. R. Technological Maturity of Aircraft-Based Methane Sensing for Greenhouse Gas Mitigation. *Environmental Science & Technology* **2024**, *58*, 9591–9600, https://doi.org/10.1021/acs.est.4c02439.

(32) OGMP 2.0 The Oil & Gas Methane Partnership 2.0. 2024; UN Environment Programme (UNEP). https://ogmpartnership.com/.

(33) Council of European Union Council regulation (EU) 2019/942 (COM(2021)0805 – C9-0467/2021 – 2021/0423(COD)). 2023; https://www.europarl.europa.eu/doceo/document/TA-9-2023-0127_EN.html.

(34) U.S. Environmental Protection Agency. *Greenhouse Gas Reporting Rule: Revisions and Confidentiality Determinations for Petroleum and Natural Gas Systems*; Final Rule 89 FR 42062, 2024; pp 42062–42327, https://www.federalregister.gov/d/2024-08988 (last accessed October 15, 2024).

(35) Donahue, C. P.; Oberoi, K.; Dillon, J.; Hengst, V.; Kennedy, B.; Kearney, W.; Lennox, J.; Rehbein, E.; Sykes, R.; Dudiak, C.; Altamura, D.; Doherty, G.; Roos, P.; Brasseur, J. K.; Thorpe, M. Aerial LiDAR Based, Source Resolved Methane Emissions Inventory: Permian Basin Case Study for Benchmarking U.S. Emissions. *EarthArXiv* **2025**, https://doi.org/10.31223/X5S45T.

(36) Chen, Y.; Sherwin, E. D.; Berman, E. S.; Jones, B. B.; Gordon, M. P.; Wetherley, E. B.; Kort, E. A.; Brandt, A. R. Quantifying Regional Methane Emissions in the New Mexico Permian Basin with a Comprehensive Aerial Survey. *Environmental Science & Technology* **2022**, *56*, 4317–4323, https://doi.org/10.1021/acs.est.1c06458.

(37) Williams, J. P. Estimated basin-level individual methane emission rates for oil and gas facilities from the continental United States in 2021. 2025; https://doi.org/10.5281/zenodo.16740519.

TOC Graphic

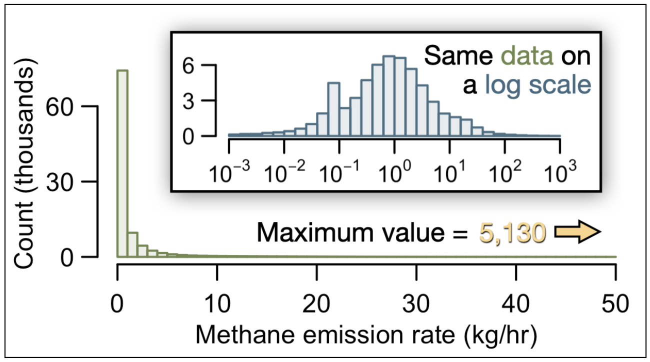
Same data on
a log scale
6
3
0
10^−3 10^−2 10^−1 10^0 10^1 10^2 10^3
Count (thousands)
60
30
0
Maximum value = 5,130
0 10 20 30 40 50
Methane emission rate (kg/hr)

Supporting Information for:

Sampling variability under extreme skewness: sample size guidance for future methane measurement campaigns

William S. Daniels[1,2] and Dorit M. Hammerling[1,3]

[1]Department of Applied Mathematics and Statistics, Colorado School of Mines, Golden, Colorado 80401, United States

[2]Current Affiliation: Department of Environmental Health and Engineering, Johns Hopkins University, Baltimore, Maryland 21218, United States

[3]Energy Emissions Modeling and Data Lab, The University of Texas at Austin, Austin, Texas 78712, United States

Email: wdanie16@jhu.edu

Contents

S1 Details on selected reference distributions

Sherwin et al. (2024) [1] provide one to five emission rate distributions per basin, each corresponding to a different measurement campaign. Williams et al. (2025) [2] provide 500 realizations of the methane emission rate distribution for each basin. These realizations are meant to represent uncertainty from their modeling framework for the emission rate distribution for 2021. Because the Sherwin distributions span multiple years, we select one Sherwin distribution per basin that most closely aligns in time with the Williams distributions. This was done instead of averaging the Sherwin distributions to mitigate the effects of temporal variability when comparing between the two studies. Table 1 lists the Sherwin distributions that were selected for use in this study.

Justification for our selection is as follows. Sherwin et al. (2024) provide only one distribution for the Appalachian, Barnette, and Uinta basins. For the Denver-Julesburg, we select the latest of the two distributions (Fall 2021). For the Permian, we select the campaign with the best coverage (Carbon Mapper 2019) over the more recent campaigns (Carbon Mapper 2020-2021). This is because we treat the Sherwin and Williams distributions as the true population distributions for their respective basins in this study, so having as large a sample helps mitigate sampling variability in our choice of population distribution. For the San Joaquin, we select the latest distribution (Fall 2021).

For all of our analysis using the Williams et al. (2025) distributions, we use the average of the 500 realizations produced by their simulation framework. To perform this average, we first sort each realization from the smallest to the largest emission. We then average the smallest emission from all 500 realizations, the second smallest emission from all 500 realizations, et cetera. This procedure works because all 500 realizations have the same length.

Table 1: Exact reference distributions used in this study.

Basin name used in this study	**Distribution from Sherwin et al. (2024)**	**Distribution from Williams et al. (2025)**
Appalachian	Carbon Mapper Pennsylvania 2021	Appalachian
Barnette	Kairos Fort Worth 2021	Barnette
Denver-Julesburg	Carbon Mapper Denver-Julesburg Fall 2021	Denver-Julesburg
Permian	Carbon Mapper Permian 2019	Permian
San Joaquin	Carbon Mapper San Joaquin Fall 2021	San Joaquin
Uinta	Carbon Mapper Uinta 2021	Uinta

S2 Distribution of sample means for each basin

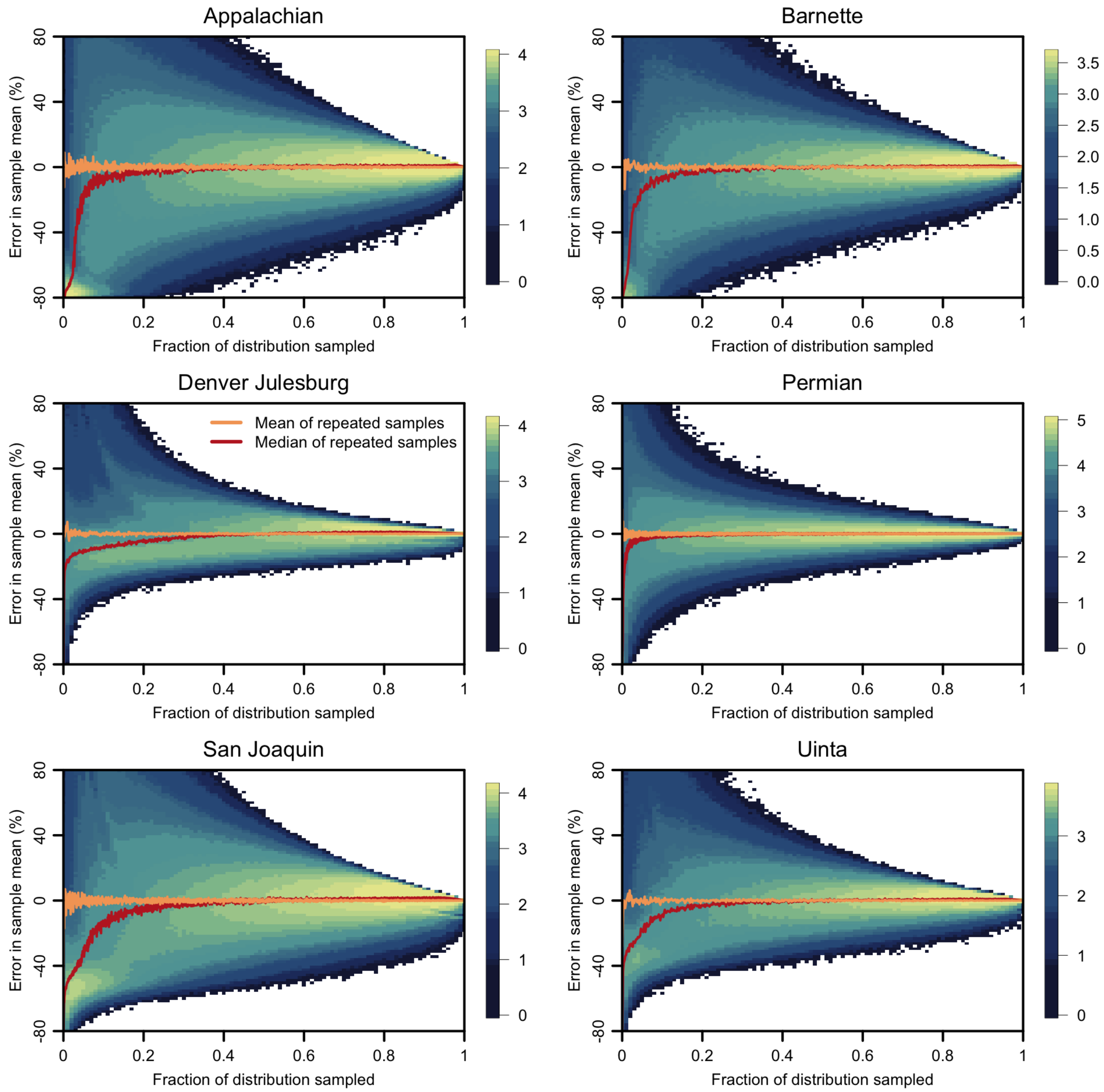

Figure S1: Distribution of sample means at different sample sizes using the Sherwin et al. (2024) [1] distributions. Vertical axis shows percent error between sample mean and true population mean. Horizontal axis shows the sample size as a percent of the length of the population distribution. Color scale shows the number of samples within each grid cell.

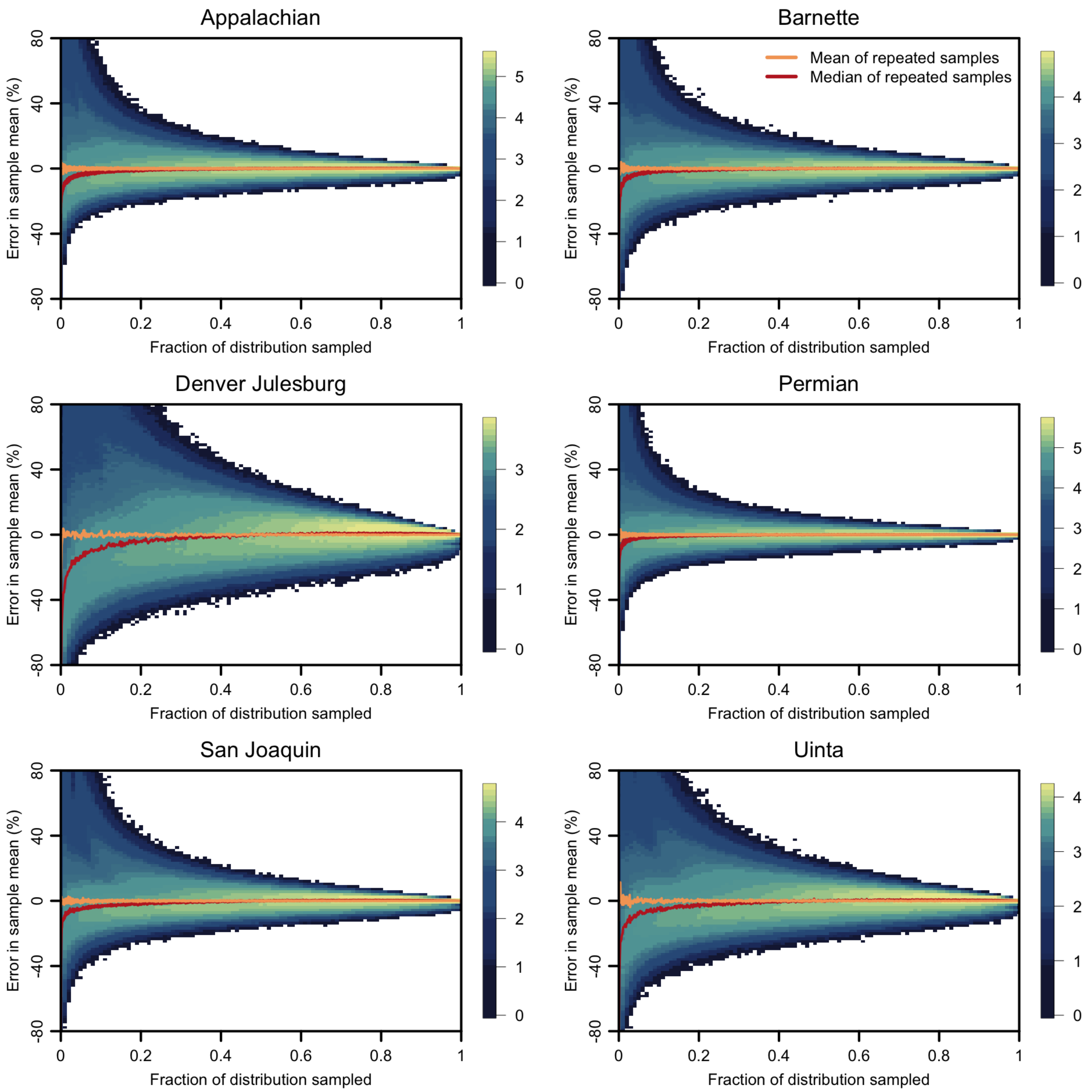

Figure S2: Distribution of sample means at different sample sizes using the Williams et al. (2025) [2] distributions. Vertical axis shows percent error between sample mean and true population mean. Horizontal axis shows the sample size as a percent of the length of the population distribution. Color scale shows the number of samples within each grid cell.

S3 Sample mean metrics at all sample sizes

Figures S3 through S14 show the sample mean error metrics used in Figure 4 in the main text evaluated at all sample sizes. See the main text for a definition of each metric. Note that sample size is expressed as a fraction of the full distribution. In all of the following plots, the light shaded lines show the metric value at every sample size, and the darker lines show the centered moving average with window size equal to 0.1% of the length of the distribution.

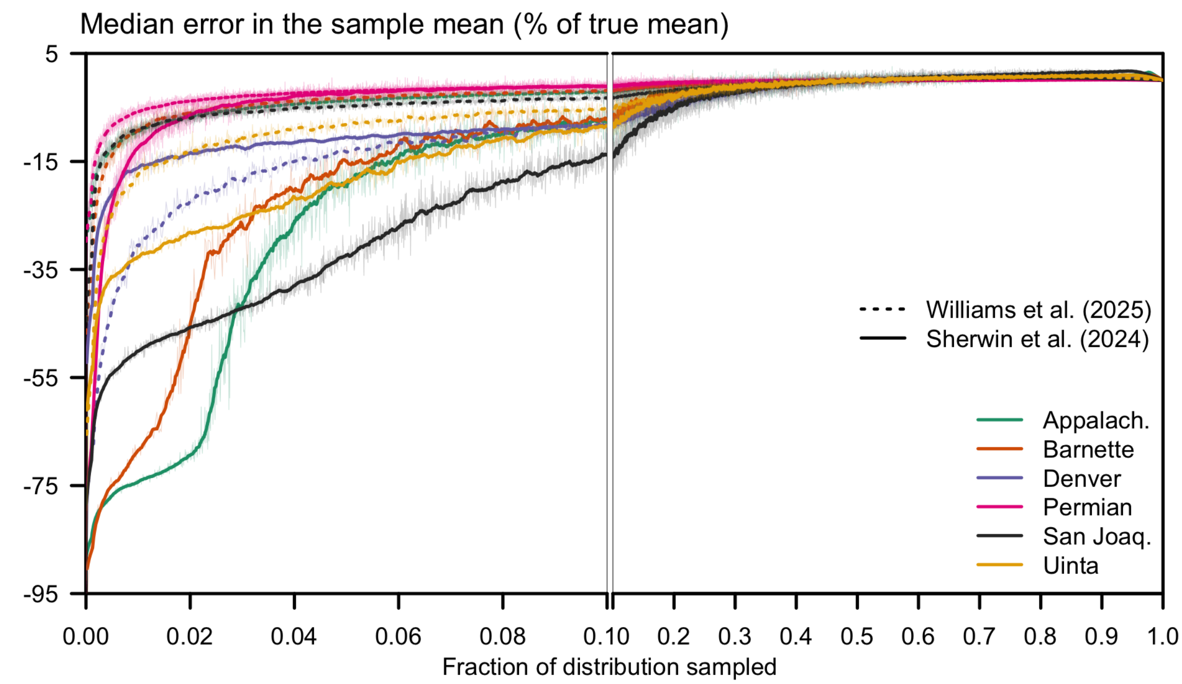

Figure S3: Median error in the sample mean as a function of sample size. Note that the horizontal axis zooms in on the [0.0, 0.1] region to show detail.

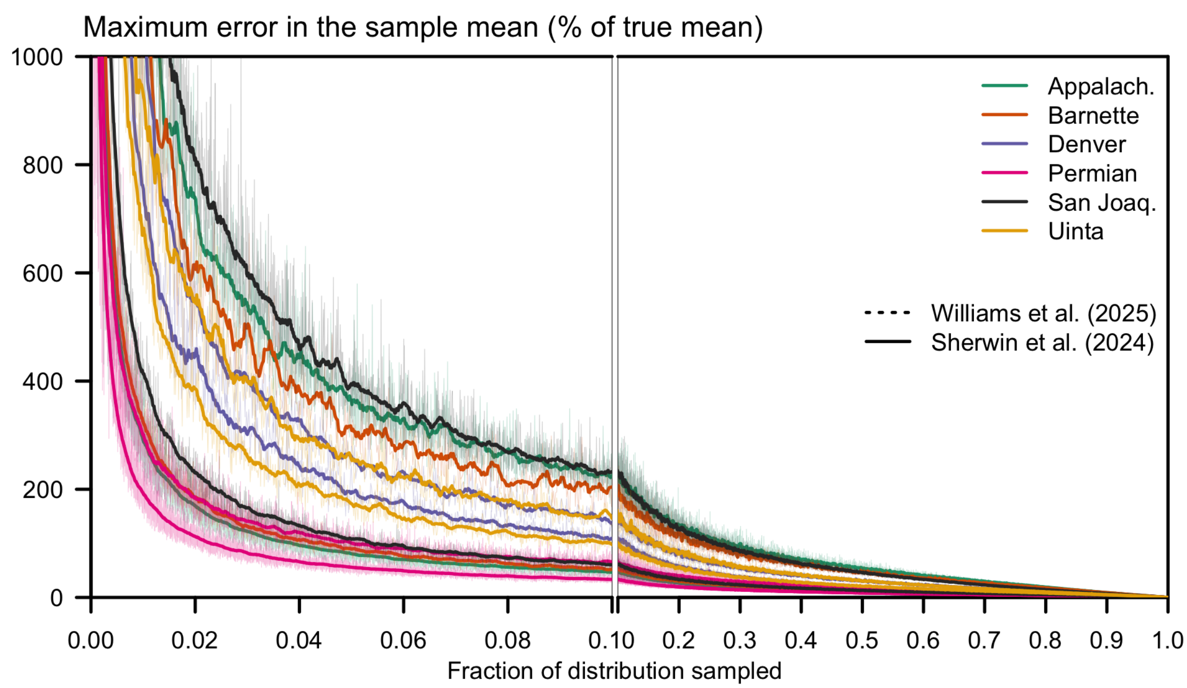

Figure S4: Maximum error in the sample mean as a function of sample size. Note that the horizontal axis zooms in on the [0.0, 0.1] region to show detail.

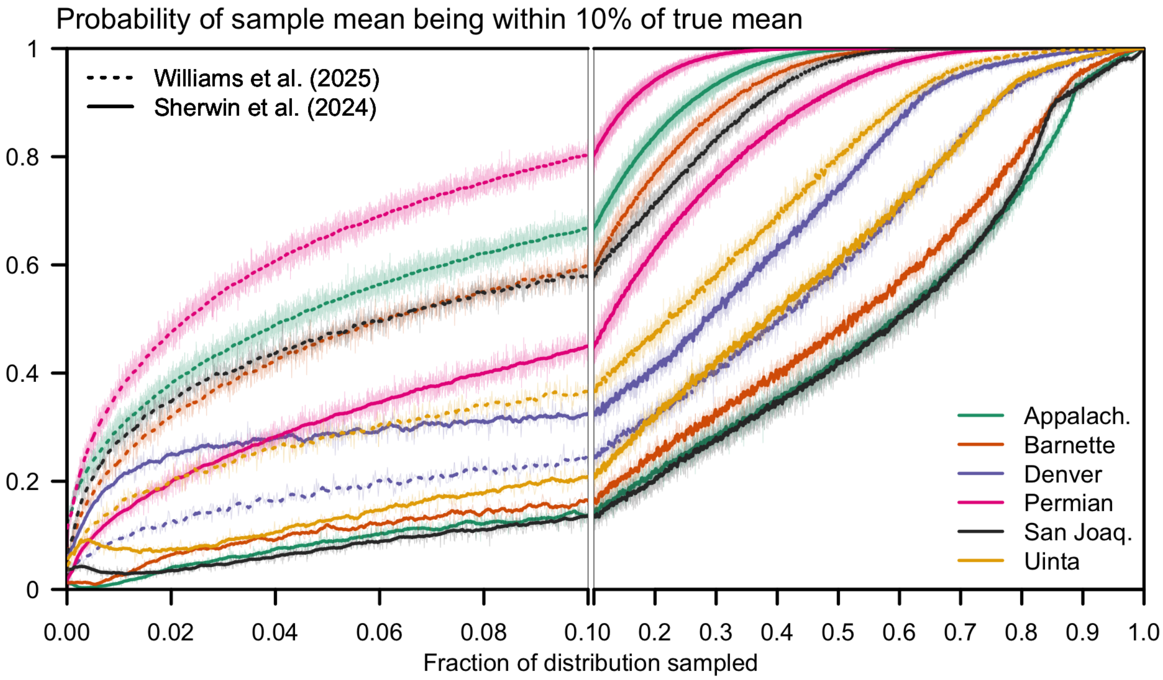

Figure S5: Probability of the sample mean having error within 10% of the true mean as a function of sample size. Note that the horizontal axis zooms in on the [0.0, 0.1] region to show detail.

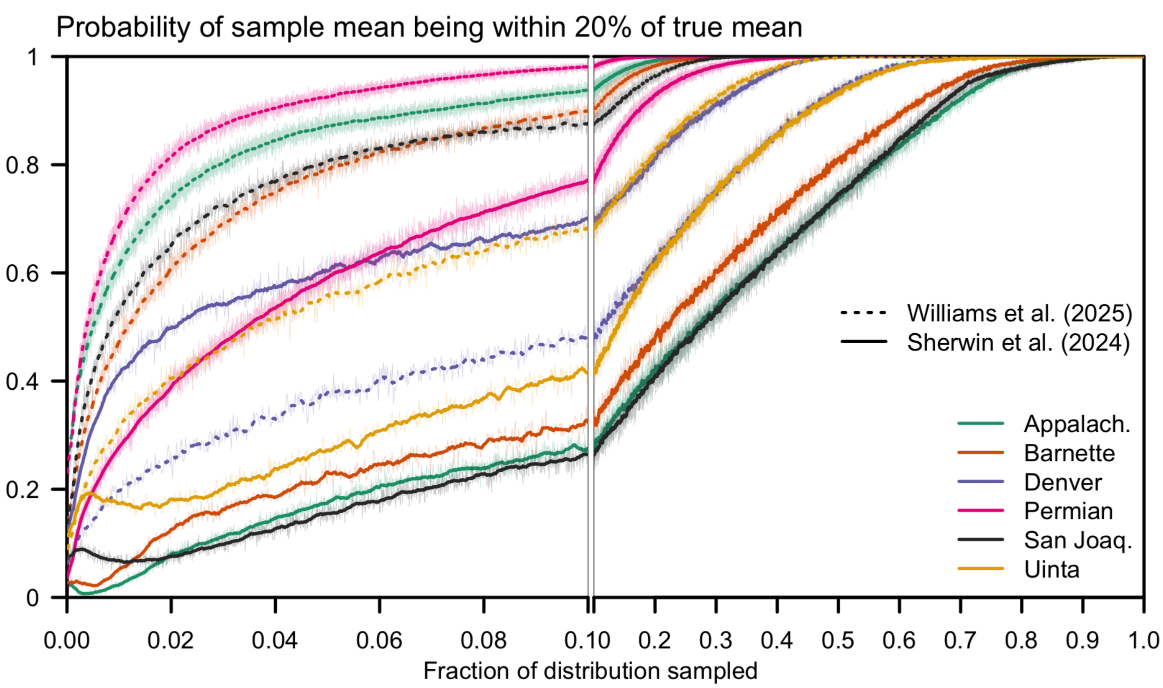

Figure S6: Probability of the sample mean having error within 20% of the true mean as a function of sample size. Note that the horizontal axis zooms in on the [0.0, 0.1] region to show detail.

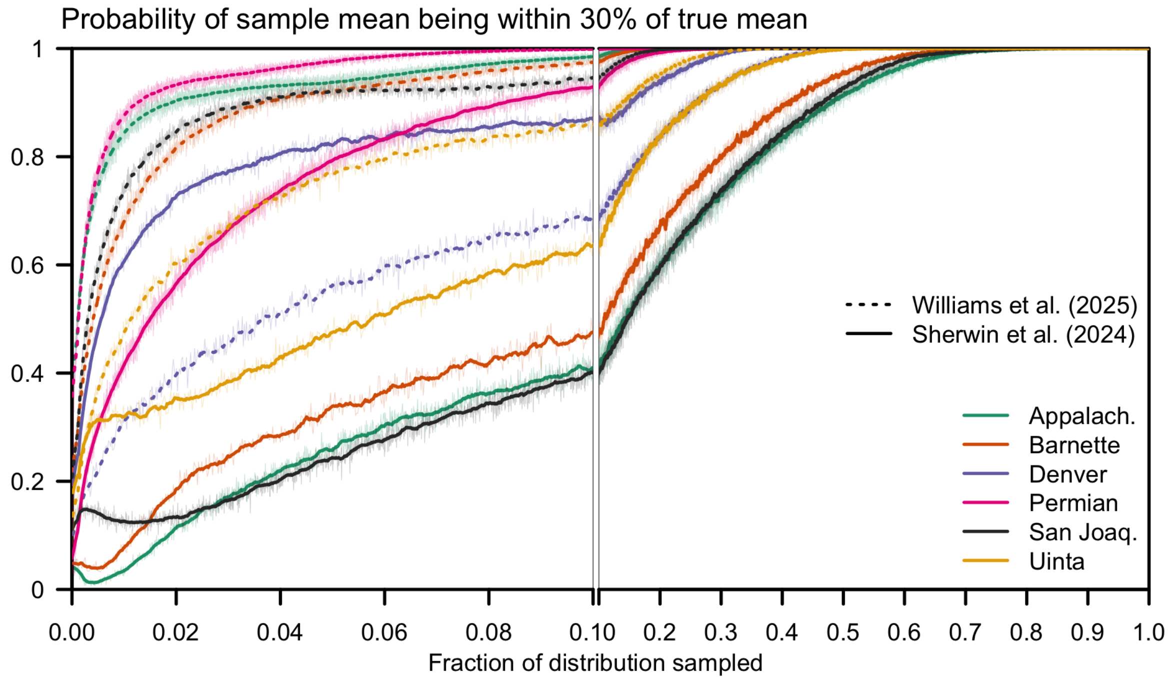

Figure S7: Probability of the sample mean having error within 30% of the true mean as a function of sample size. Note that the horizontal axis zooms in on the [0.0, 0.1] region to show detail.

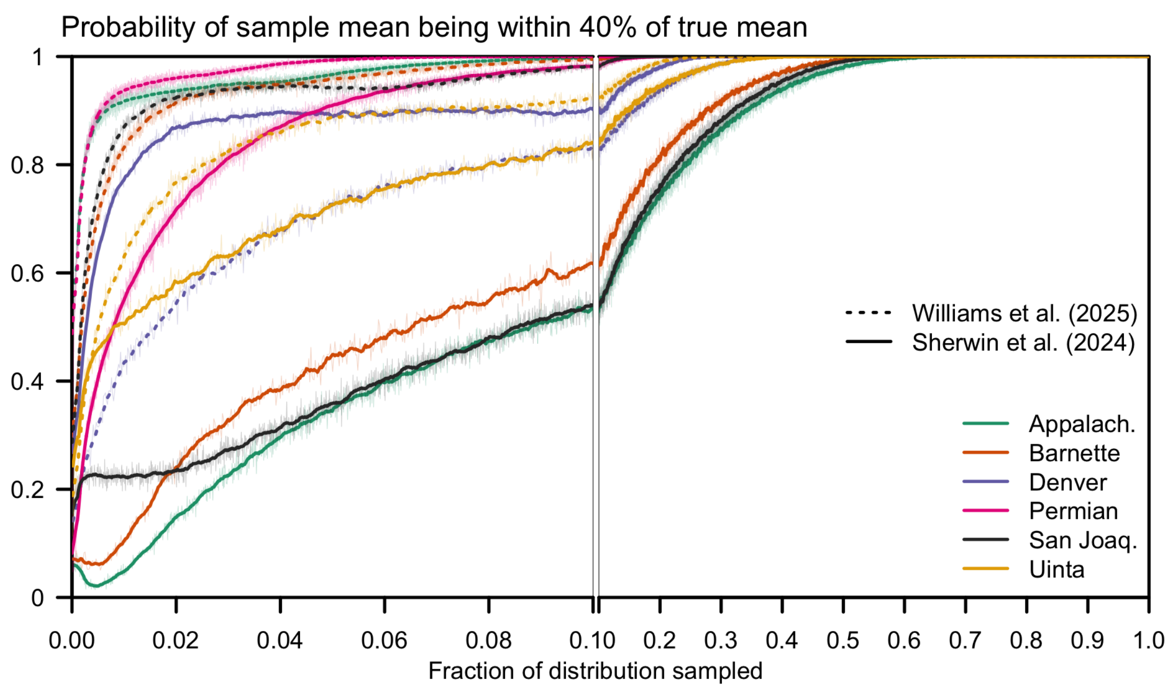

Figure S8: Probability of the sample mean having error within 40% of the true mean as a function of sample size. Note that the horizontal axis zooms in on the [0.0, 0.1] region to show detail.

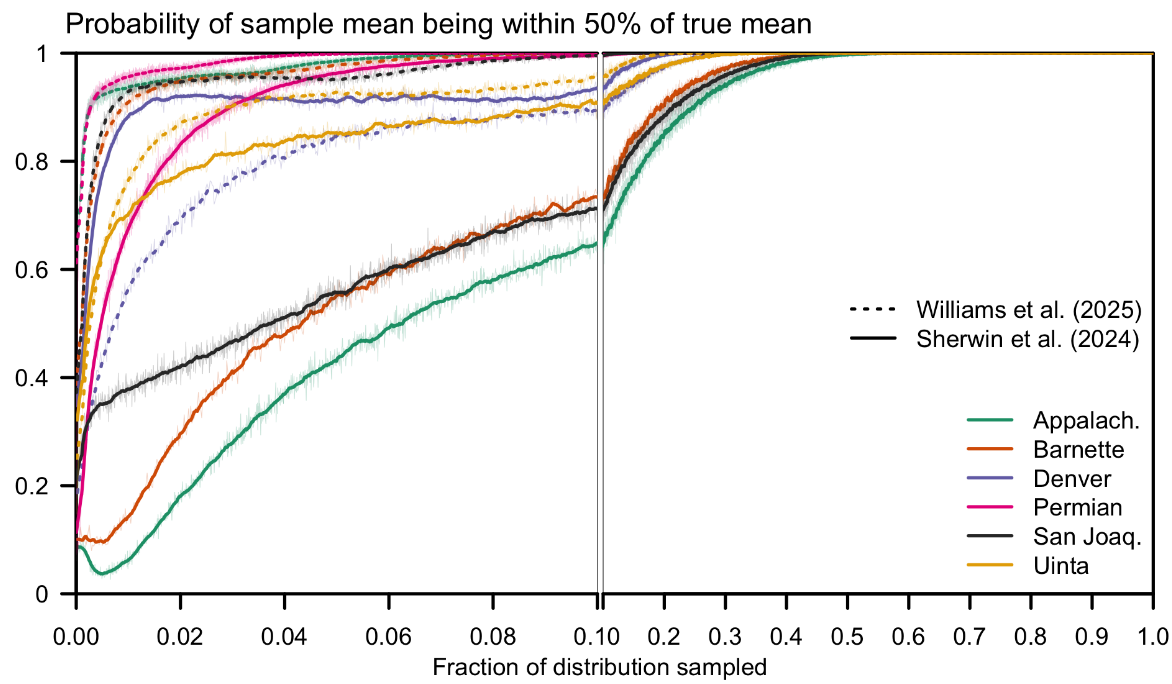

Figure S9: Probability of the sample mean having error within 50% of the true mean as a function of sample size. Note that the horizontal axis zooms in on the [0.0, 0.1] region to show detail.

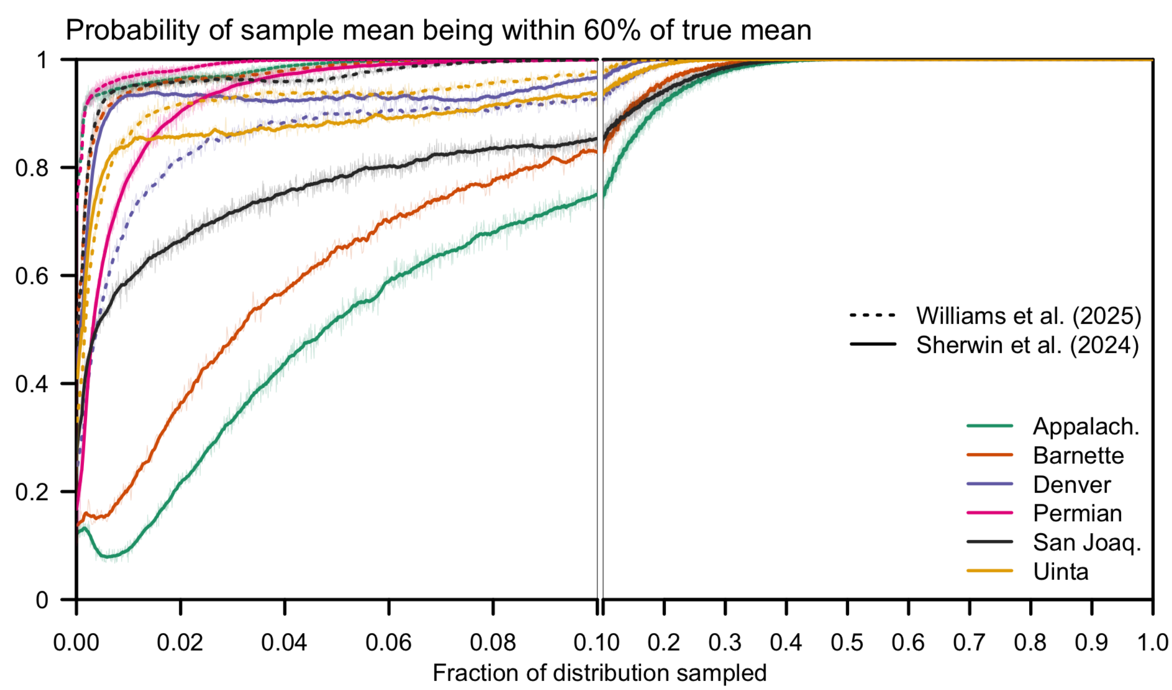

Figure S10: Probability of the sample mean having error within 60% of the true mean as a function of sample size. Note that the horizontal axis zooms in on the [0.0, 0.1] region to show detail.

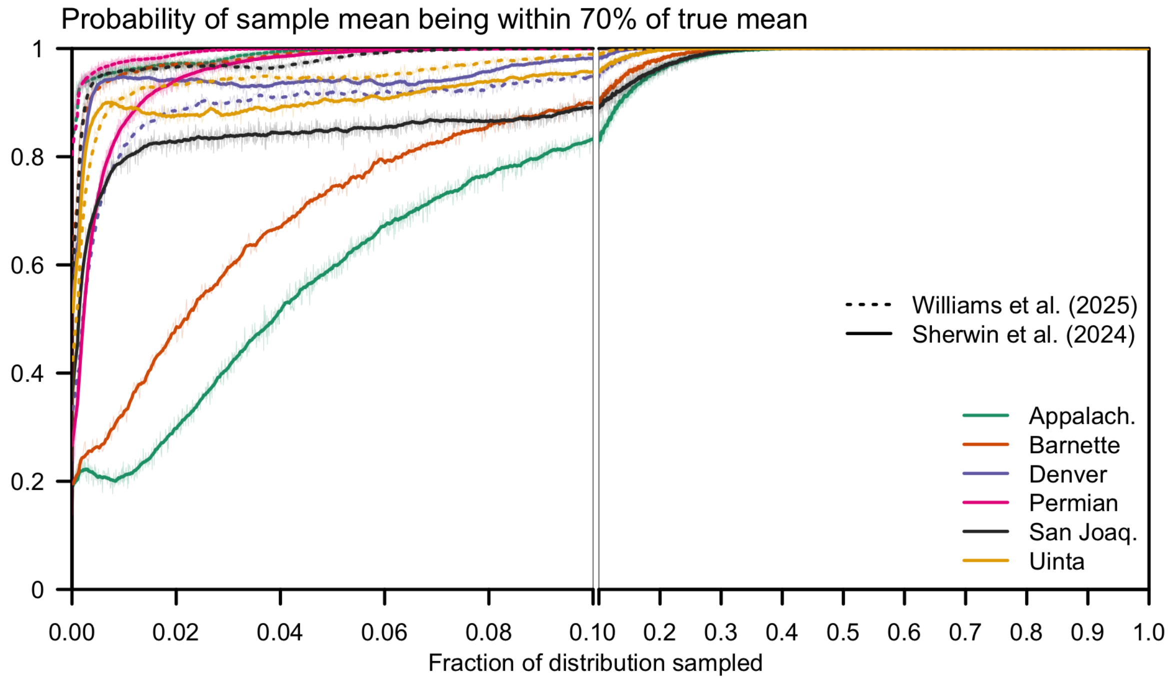

Figure S11: Probability of the sample mean having error within 70% of the true mean as a function of sample size. Note that the horizontal axis zooms in on the [0.0, 0.1] region to show detail.

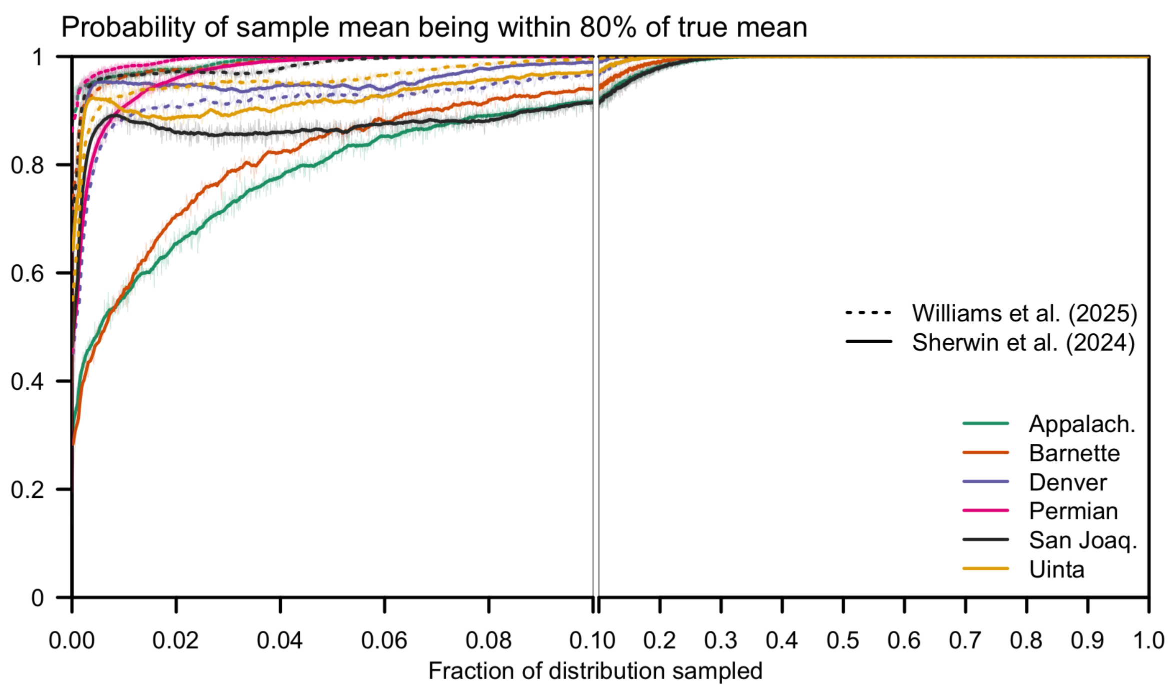

Figure S12: Probability of the sample mean having error within 80% of the true mean as a function of sample size. Note that the horizontal axis zooms in on the [0.0, 0.1] region to show detail.

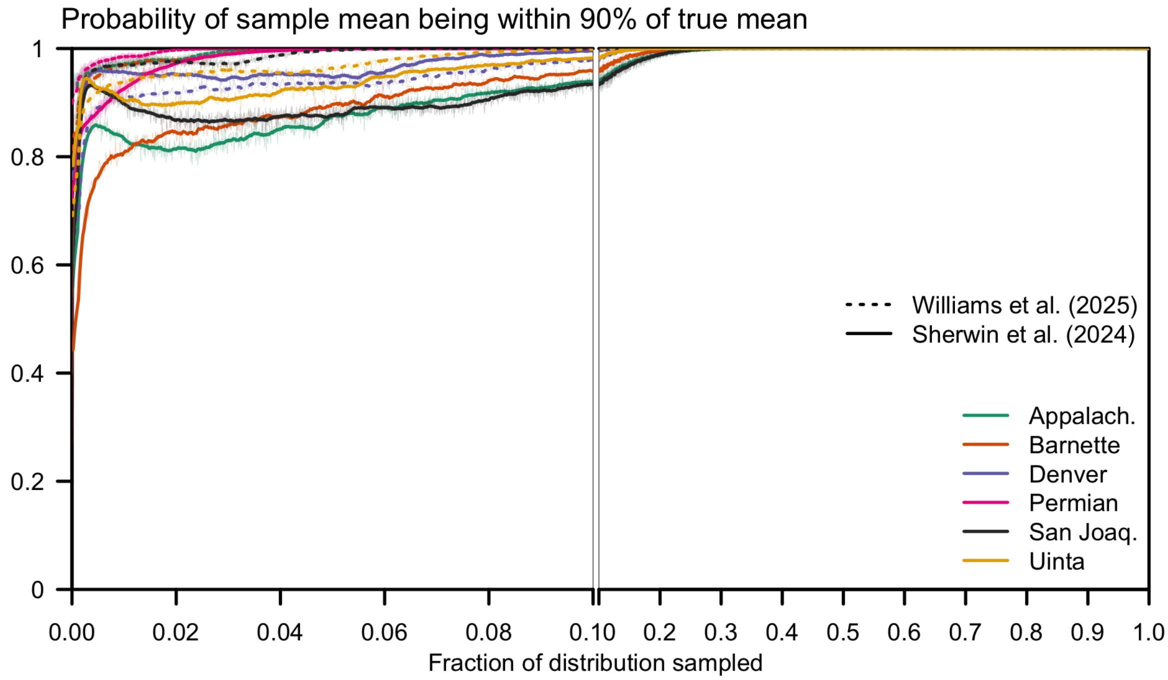

Figure S13: Probability of the sample mean having error within 90% of the true mean as a function of sample size. Note that the horizontal axis zooms in on the [0.0, 0.1] region to show detail.

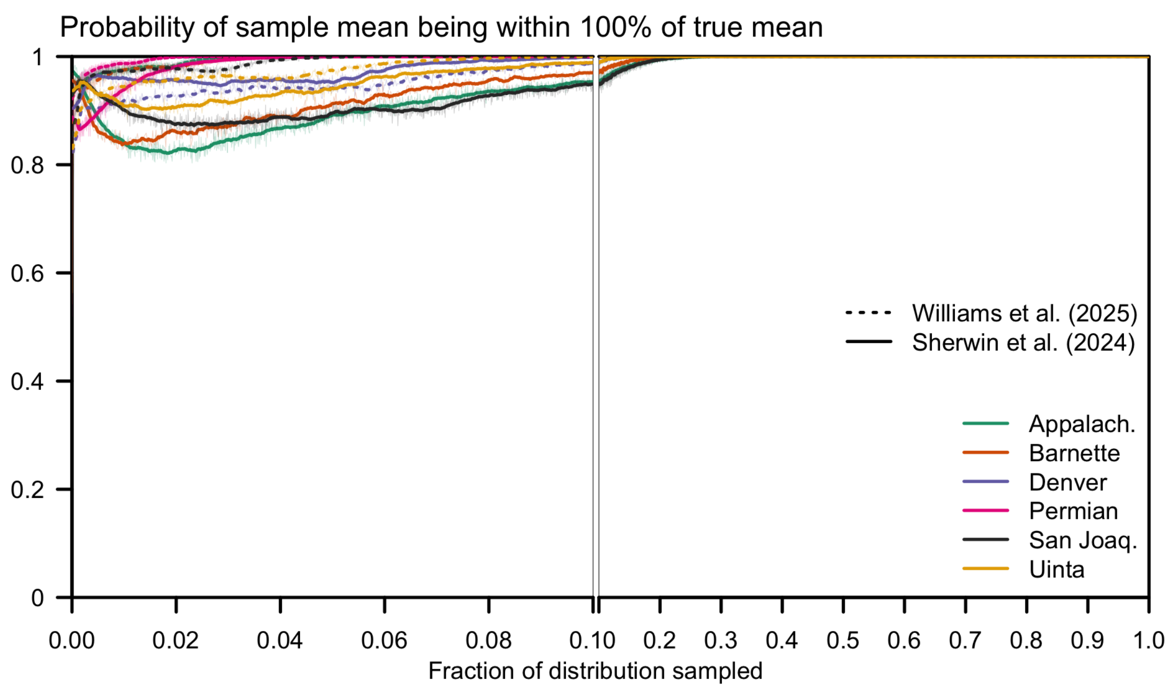

Figure S14: Probability of the sample mean having error within 100% of the true mean as a function of sample size. Note that the horizontal axis zooms in on the [0.0, 0.1] region to show detail.

References

[1] E. D. Sherwin, J. S. Rutherford, Z. Zhang, Y. Chen, E. B. Wetherley, P. V. Yakovlev, E. S. F. Berman, B. B. Jones, D. H. Cusworth, A. K. Thorpe, A. K. Ayasse, R. M. Duren, and A. R. Brandt, "US oil and gas system emissions from nearly one million aerial site measurements," *Nature*, vol. 627, pp. 328–334, Mar. 2024. https://doi.org/10.1038/s41586-024-07117-5.

[2] J. P. Williams, M. Omara, A. Himmelberger, D. Zavala-Araiza, K. MacKay, J. Benmergui, M. Sargent, S. C. Wofsy, S. P. Hamburg, and R. Gautam, "Small emission sources in aggregate disproportionately account for a large majority of total methane emissions from the US oil and gas sector," *Atmospheric Chemistry and Physics*, vol. 25, pp. 1513–1532, Feb. 2025. https://doi.org/10.5194/acp-25-1513-2025.